



**HAL**  
open science

## Clay mineral evidence of nepheloid layer contributions to the Heinrich layers in the northwest Atlantic

Viviane Bout-roumazeilles, Elsa Cortijo, Laurent Labeyrie, Pierre Debrabant

### ► To cite this version:

Viviane Bout-roumazeilles, Elsa Cortijo, Laurent Labeyrie, Pierre Debrabant. Clay mineral evidence of nepheloid layer contributions to the Heinrich layers in the northwest Atlantic. *Palaeogeography, Palaeoclimatology, Palaeoecology*, 1999, 146 (1-4), pp.211-228. 10.1016/S0031-0182(98)00137-0 . hal-02958607

**HAL Id: hal-02958607**

**<https://hal.science/hal-02958607>**

Submitted on 27 Jul 2021

**HAL** is a multi-disciplinary open access archive for the deposit and dissemination of scientific research documents, whether they are published or not. The documents may come from teaching and research institutions in France or abroad, or from public or private research centers.

L'archive ouverte pluridisciplinaire **HAL**, est destinée au dépôt et à la diffusion de documents scientifiques de niveau recherche, publiés ou non, émanant des établissements d'enseignement et de recherche français ou étrangers, des laboratoires publics ou privés.

# 1 Clay mineral evidence of nepheloid layer contributions to the Heinrich 2 layers in the northwest Atlantic

3  
4 Viviane Bout-Roumazeilles <sup>a,\*</sup>, Elsa Cortijo <sup>b</sup>, Laurent Labeyrie <sup>b,c</sup>, Pierre Debrabant <sup>d</sup>

5  
6 a Faculteit der Aardwetenschappen, Vrije Universiteit Amsterdam, De Boelelaan 1085, 1081  
7 HV Amsterdam, The Netherlands

8 \* Corresponding author.

9 b Centre des Faibles Radioactivités, laboratoire mixte CNRS-CEA, 91 198 Gif-sur-Yvette,  
10 France

11 c Département des Sciences de la Terre, bât. 504, Université de Paris Sud, 91 045 Orsay,  
12 France

13 d Laboratoire de Sédimentologie et Géodynamique, URA 719 CNRS, Université de Lille 1,  
14 59 655 Villeneuve d'Ascq, France

15  
16 **Keywords:** North Atlantic; clay minerals; nepheloid layer; Pleistocene

## 17 18 **Abstract**

19 The clay fraction of four cores drilled in the north Atlantic Ocean was studied at a  
20 very high resolution over the last 150 ka in order to record the mineralogical signature of  
21 Heinrich events. Factor analysis of clay mineralogy establishes that three independent factors  
22 represent the main variations: a 'detrital factor' (illite C chlorite C kaolinite), a 'smectite  
23 factor', and a 'mixed-layer factor' (IVML: illite-vermiculite mixed-layered clay). The clay  
24 mineral fraction of core SU90-38 drilled in the northeastern Atlantic basin did not record any  
25 Heinrich event, whereas large changes in the clay mineral fraction occurred during Heinrich  
26 events H1, H2, H4, and H5 in the three cores from the northwestern Atlantic basin (cores  
27 SU90-08, SU90-11, and SU90-12). Heinrich layers are characterized by increases in the  
28 detrital factor in cores SU90-08 and SU90-11, and sharp increases in the mixed-layer factor in  
29 cores SU90-11 and SU90-12. The geographical setting of the cores, the pattern of surface,  
30 intermediate and deep water circulation, and the main sources of clay minerals allow  
31 recognition of two major mechanisms involved in the deposition of the Heinrich Layers: (1)  
32 an increased supply of detrital clay minerals by the icebergs; and (2) a specific input of illite-  
33 vermiculite mixed-layer clay minerals by a nepheloid layer.

34

## 35 **1. Introduction**

36 High-resolution palaeoceanographic studies in the North Atlantic Ocean provide much  
37 evidence of massive fluxes of coarse detrital material that are interpreted as a consequence of  
38 abrupt climatic changes. The Heinrich layers corresponds to short periods of very high  
39 sedimentation rates. These 'Heinrich layers' mainly occur within a preferential accumulation  
40 belt, between 40 and 50°N, along the edge of the polar front (Ruddiman, 1977; Heinrich,  
41 1988; Bond et al., 1992; Broecker et al., 1992; Grousset et al., 1993). These events are also  
42 characterized by decreases in the number of species and abundance of foraminifers, the  
43 resulting assemblages being dominated by the cold species *N. pachyderma* (left coiling)  
44 (Bond et al., 1992). A high content of detrital carbonate, especially dolomite, suggests that  
45 most of the terrigenous material originates from the eastern margin of the Laurentide ice-sheet  
46 (Andrews and Tedesco, 1992; Huon and Ruch, 1992; Andrews et al., 1994). Heinrich events  
47 are generally closely associated with instabilities of the Laurentide ice-sheet. MacAyeal  
48 (1993) suggested that the Heinrich events were caused by free oscillations of the Laurentide  
49 ice-sheet: when the frozen sediments, at the base of the ice-sheet, started to thaw, they formed  
50 a lubricant and the ice-sheet began to slip. Ice flow from Hudson Bay may have delivered  
51 coarse particles (between 150 µm and several millimetres), eroded from the calcareous  
52 Paleozoic bedrock, to the continental slope and to the deep oceanic basin. Debris flows,  
53 turbidity currents, and intermediate water masses may also be involved in producing the  
54 Heinrich layers. This is evident from the high accumulation rates observed in sediments  
55 sampled outside the main icebergs pathways (Andrews and Tedesco, 1992). Here we used  
56 clay particles (<2 µm) which are easily transported by oceanic currents, to demonstrate the  
57 contribution of a nepheloid layer to the Heinrich layer deposits in the northwestern Atlantic  
58 basin.

59

## 60 **2. Material and methods**

### 61 *2.1. Core settings*

62 Four sediment cores from the cruise Paleocinat I in 1990 were studied: SU90-08,  
63 SU90-11, SU90-12, and SU90-38 (Table 1; Fig. 1). Three cores were taken from the  
64 northwestern Atlantic basin: the southernmost core SU90-08 is located at 43°N near the  
65 Azores, on the western flank of the mid-oceanic ridge at 3080 m depth, in a quiet deep  
66 environment; core SU90-11 (3645 m) and SU90-12 (2950 m) are situated on seamounts at 44  
67 and 51°N, respectively, near the entrance of the Labrador Sea. Cores SU90-11 and SU90-12

68 are situated on seamounts at 1000 m above the sea-floor: sedimentation at these sites is  
69 therefore only controlled by intermediate or/and surface water masses flowing out the  
70 Labrador sea. Core SU90-38 was sampled in the northeastern Atlantic basin, at 54°N, near  
71 Rockall Plateau, at 2900-m water depth. This site is under the influence of the eastern drift of  
72 the North Atlantic Deep Water overflowing the Wyville–Thomson rise, and by surface water  
73 masses originating from the Greenland and Norwegian seas.

74

## 75 *2.2. Correlation and chronology*

76 The age model for each site is based on a comparison between the benthic and/or  
77 planktonic  $\delta^{18}\text{O}$  records and the spectral mapping SPECMAP stack (Martinson et al., 1987)  
78 using the Analyseries software (Paillard et al., 1996). A linear interpolation was applied  
79 between the stratigraphic levels identified (Table 2), assuming that the sedimentation rate was  
80 constant between these levels. The age–depth relations are given in Table 2 and shown in Fig.  
81 2. The oxygen isotope analysis of foraminifers was measured on an automatic carbonate  
82 preparation line coupled to a Finnigan MAT 251 mass spectrometer (Centre des Faibles  
83 Radioactivités, Gif-sur-Yvette, France) Isotopic stages and their boundaries were deduced  
84 from isotopic curves, magnetic susceptibility, and reflectance (Grousset et al., 1993; Cortijo et  
85 al., 1995). The mean sedimentation rate of core SU90-08 is about 4.2 cm/ka<sup>-1</sup> and varies along  
86 the series (Fig. 2). The sedimentation rate is higher in the upper part of the core (0–107.6 ka),  
87 5.3 cm/ ka<sup>-1</sup>, and between 183.4 and 225.2 ka, where it reaches 6.2 cm/ ka<sup>-1</sup>. Core SU90-11  
88 records slower sedimentation rates than core SU90-08: the mean value is of 2.9 cm/ ka<sup>-1</sup> (Fig.  
89 3). The highest rates in this core are observed in the upper part (0–122.2 ka), 3.8 cm/ ka<sup>-1</sup>.  
90 Core SU90-12 has the slowest and most regular sedimentation rate, with a mean value of 2.9  
91 cm/ ka<sup>-1</sup> (Fig. 3). The mean ages (Fig. 2) for the Heinrich layers (14.5 ka for H1, 22 ka for  
92 H2, 27 ka for H3, 40 ka for H4, 50 ka for H5, and 60 ka for H6) are deduced from the age  
93 model for core SU90-08 (Grousset et al., 1993).

94

## 95 *2.3. Method of clay analysis*

96 All samples were first decalcified with 0.2 N hydrochloric acid. The excess acid was  
97 removed by repeated centrifugations. The clay-sized fraction (<2  $\mu\text{m}$ ) was isolated by settling,  
98 and oriented on glass slides (oriented mounts). Three XRD (X-ray diffraction) determinations  
99 were performed: (a) untreated sample; (b) glycolated sample (after saturation for 12 h in  
100 ethylene glycol); and (c) sample heated at 490°C for two hours (Holtzapffel, 1985). The  
101 analyses were run on a Philips PW 1710 X-ray diffractometer, between 2.49 and 32.5°2 $\theta$ .

102 Each clay mineral is then characterized by its layer plus interlayer interval as revealed  
103 by XRD analysis. Smectite is characterized by a peak at 14 Å on the untreated sample test,  
104 which expands to 17 Å after saturation in ethylene-glycol and retracts to 10 Å after heating.  
105 Illite presents a basal peak at 10 Å on the three tests (natural, glycolated, and heated). The  
106 IVML (illite-vermiculite mixed-layered clay) is determined by a peak at 12 Å which does not  
107 expand after saturation in ethylene-glycol and retracts to 10 Å after heating. Chlorite is  
108 characterized by peaks at 14, 7, 4.72, and 3.53 Å on the three tests. Kaolinite is characterized  
109 by peaks at 7 and 3.57 Å on the untreated sample and after saturation in ethylene glycol. Both  
110 peaks disappear or are strongly reduced after heating. Semi-quantitative estimation of clay  
111 minerals abundances has been done according to the method detailed in Holtzapffel (1985).

112 The reproducibility of technical works and measurements was tested: 5 oriented  
113 mounts prepared from the same samples were submitted 3 times to XRD. The relative error is  
114  $\pm 5\%$ .

115

#### 116 *2.4. Method of factor analysis*

117 Factor analysis has been performed on all clay abundance data. The method used the  
118 Principal Component Analysis (PCA) by the orthogonal transformation method (Johnson and  
119 Wichern, 1982; Albarède, 1995). The PCA explains the covariance structure of multivariate  
120 data through a reduction of the whole data to a smaller number of independent variables,  
121 called factors.

122

### 123 **3. Results**

124

#### 125 *3.1. General data and clay mineralogy*

126

##### 127 *3.1.1. Core SU90-08*

128 Sediments of core SU90-08 are mainly composed of gray to dark gray carbonate  
129 (foraminifera and nannofossil) oozes and muds interbedded with terrigenous muddy clay,  
130 silty mud and terrigenous mud (sand, silt and clay-sized particles mixed together). The clay  
131 mineral association is mainly composed of illite (37 ± 7%) and smectite (33 ± 11%). Chlorite  
132 and kaolinite are less abundant with respectively 14% ( $\pm 3\%$ ) and 11% ( $\pm 3\%$ ) of the clay  
133 mineral association (Table 3). The random IVML constitutes less than 5% of clay minerals  
134 association (Bout- Roumazeilles, 1995). The Heinrich layers, which are characterized by their  
135 high coarse-size detrital content (calcite, dolomite, quartz, feldspars and amphiboles) are

136 significantly enriched in illite (Table 4), which reaches 55% of the clay mineral association.  
137 The content of chlorite (20%) and kaolinite (15%) also increases in these layers, whereas  
138 smectite sharply decreases (10%).

139

#### 140 *3.1.2. Core SU90-11*

141 Sediments of core SU90-11 are composed of dark gray terrigenous muds interbedded  
142 with gray carbonate (nannofossils with foraminifera) muds. The clay mineral association is  
143 dominated by illite (average value of  $34 \pm 4\%$ ), with 17% ( $\pm 7\%$ ) IVML and 20% ( $\pm 4\%$ )  
144 chlorite. Smectite and kaolinite represent 16% ( $\pm 7\%$ ) and 12% ( $\pm 2\%$ ) of the clay mineral  
145 association, respectively (Table 3). The Heinrich layers are characterized by high magnetic  
146 susceptibility, high detrital carbonate content, by a strong increase in IVML in the clay-size  
147 fraction, which reach 28% of the clay mineral association and absence of smectite. The  
148 percentages of chlorite and kaolinite remain stable.

149

#### 150 *3.1.3. Core SU90-12*

151 The sediments of core SU90-12 are mainly composed of dark gray terrigenous muds,  
152 interbedded with minor levels of carbonate (nannofossils with foraminifera) muds. On the  
153 average, the clay fraction is dominated by mean values of 34% ( $\pm 5\%$ ) illite and 21% (4%)  
154 chlorite (Table 3). The IVML represents 18% ( $\pm 8\%$ ) of the clay mineral association.  
155 Smectite ( $15 \pm 8\%$ ) and kaolinite ( $12 \pm 2\%$ ) are less abundant (Bout-Roumazeilles,  
156 1995). The Heinrich layers are characterized by high contents of IVML, which reach  
157 32% of the clay mineral association and by low contents of smectite (8%). The content  
158 of illite, chlorite, and kaolinite slightly decreases within the Heinrich layers.

159

#### 160 *3.1.4. Core SU90-38*

161 Core SU90-38 is composed of dark gray terrigenous muddy clay, of gray carbonate  
162 mud, and of carbonate (foraminifera with nannofossils) oozes interbedded with minor beds of  
163 silt and fine sand. The clay mineral association mostly includes illite ( $39 \pm 7\%$ ) and smectite  
164 ( $35 \pm 11\%$ ). Chlorite ( $14 \pm 3\%$ ) and kaolinite ( $12 \pm 2\%$ ) are less abundant whereas the random  
165 illite-smectite mixed-layer minerals occur as trace amounts (Table 3). No significant  
166 modification of the clay association is observed in the Heinrich layers (Heinrich layers have  
167 been distinguished on the basis of their high detrital content). Illite ( $42 \pm 5\%$ ) and smectite  
168 ( $32 \pm 4\%$ ) still constitute the main part of the clay mineral association, and chlorite ( $14 \pm 2\%$ )  
169 and kaolinite ( $12 \pm 3\%$ ) are less abundant.

170 In summary, the mean percentages of illite, chlorite, and kaolinite are essentially  
171 constant in the four cores. Illite, chlorite, and kaolinite represent 62% (core SU90-08) to 67%  
172 (core SU90-12) of the clay mineral association. Abundant IVML characterizes the clay  
173 mineral association of the western cores SU90-11 (17%) and SU90-12 (18%), whereas it is  
174 absent from the two other cores. Low abundances of smectite characterized western cores  
175 SU90-11 and SU90-12 where it constitutes only 15% of the clay mineral association. In  
176 contrast smectite constitutes more than 30% of the clay mineral fraction in cores SU90-08 and  
177 SU90-38. In core SU90-08, the Heinrich layers are characterized by high contents of illite,  
178 chlorite, and kaolinite (up to 90% of the clay mineral association), whereas smectite strongly  
179 decreases. In cores SU90-11 and SU90-12, abundant IVML (up to 32%) characterizes the  
180 Heinrich layers. Smectite disappears in the Heinrich layers of core SU90-11, and is strongly  
181 reduced in core SU90-12. There is no coherent variation of illite, chlorite, and kaolinite within  
182 the Heinrich layers: illite, chlorite, and kaolinite increase in core SU90-11, decrease in core  
183 SU90-12, and strongly increase in core SU90-08. In core SU90-38, the clay mineralogy of the  
184 Heinrich layers is not different from the rest of the core.

185

### 186 *3.2. Results of the correlation matrix*

187

#### 188 *3.2.1. Core SU90-08*

189 The correlation matrix of core SU90-08 (Table 5) indicates that the variations in  
190 chlorite, illite, and kaolinite abundances are very well correlated ( $0.7 < r < 0.8$ ). Smectite  
191 abundances appear to be independent of the other minerals. The principal component analysis  
192 reveals that two factors represent the major variations ( $0.9 < \text{factor scores} < 1$ ) in all four clay  
193 minerals (Table 6). One factor (the 'ICK factor') groups together illite, chlorite, and kaolinite,  
194 whereas the other one corresponds to smectite ('smectite factor'). The primary  
195 intercorrelation indicates that the two factors ( $r = 0$ ) are independent.

196

#### 197 *3.2.2. Core SU90-11*

198 In core SU90-11, the variations of chlorite, illite, and kaolinite are well correlated ( $r =$   
199  $0.8$ ). They are grouped (Table 6) together in the 'detrital factor' (factor scores =  $0.9$ ). The  
200 correlation matrix (Table 5) indicates that smectite and IVML are slightly anticorrelated ( $r =$   
201  $0.6$ ). Consequently, the primary intercorrelation reveals that the 'detrital factor' is not linked  
202 with the two others, whereas the 'smectite factor' and the 'mixed-layer factor' are not totally  
203 independent ( $r = 0.4$ ).

204

### 205 3.2.3. Core SU90-12

206 The results of the factor analysis of core SU90-12 are approximately similar to those  
207 of core SU90-08. Once again, the variations of chlorite, of illite, and of kaolinite are well  
208 correlated and are represented by the ‘detrital factor’ (Tables 5 and 6). The correlation  
209 indexes between smectite and the other mineral are higher than in the cores SU90-08 and  
210 SU90-11, but still below the confidence level. As a result, the intercorrelation reveals that the  
211 factors are not strictly independent even if the intercorrelation index remains below the  
212 confidence level ( $-0.5 < r < 0.5$ ).

213

### 214 3.2.4. Core SU90-38

215 Correlation between the variations of chlorite, illite, and kaolinite for core SU90-38 is  
216 very high ( $0.8 < r < 0.9$ ). The variations in smectite are not significantly correlated with those  
217 of the other clay minerals (Table 5). The ‘detrital factor’ represents the main variations of  
218 illite, of chlorite, and of kaolinite (factor scores = 0.9) and the ‘smectite factor’ represents the  
219 variations of smectite (factor score = 1).

220 Overall, the variations of illite, chlorite, and kaolinite in all the cores studied are  
221 represented by the ‘detrital factor’. The variations in smectite are represented by the ‘smectite  
222 factor’ and these of the IVML by the ‘mixed-layer factor’. Below we will discuss the  
223 variations of each factor before, during, and after the Heinrich events H1 to H6.

224

## 225 3.3. Results of the factor analysis

226

### 227 3.3.1. Core SU90-08

228 The ‘detrital factor’ is low from 130 to 70 ka and shows little variations except during  
229 the Heinrich events (Fig. 4). It increases very slightly during H6 and H3, whereas it increases  
230 sharply and reaches its maximum values during H5, H4, H2, and H1. The ‘smectite factor’  
231 varies a lot during the last 130 ka. Its variations during all Heinrich events are not similar: in  
232 H6 and H3, the smectite factor increases, whereas it slightly decreases in H5, H4, H2, and H1.

233

### 234 3.3.2. Core SU90-11

235 The ‘detrital factor’ remains stable and low between 130 and 70 ka. An increase in the  
236 factor characterizes H5, H4, H2, and H1, whereas the factor does not change during H6 and  
237 H3 (Fig. 5). After H5, H4, H2, and H1, it returns to its mean level. There is no coherent

238 variation of the ‘smectite factor’ during the Heinrich events. It remains stable during H6, H5,  
239 H3, and H2, increases in H1, and decreases in H4. The ‘mixed-layer ’ factor remains stable  
240 from 130 to 70 ka, and during H6 and H3, but shows very short increases during H5, H4, H2,  
241 and H1.

242

### 243 3.3.3. Core SU90-12

244 Major variations of the ‘detrital factor’ occur between 130 and 70 ka, whereas it  
245 remains relatively stable between 35 and 0 ka (Fig. 5). Heinrich events H6, H5, and H4 are  
246 characterized by increases of this factor, the most important variations being found in H5 and  
247 H4. Between 130 and 70 ka, the ‘smectite factor’ shows marked variations. Over the past 70  
248 ka this factor is mostly characterized by decreases during H5, H4, and H2. The variations of  
249 the ‘mixed layer factor’ are similar to those of core SU90-11: the mixed-layer factor increases  
250 abruptly at the beginning of each Heinrich event, and then drops to below average values.  
251 This is especially obvious for H5 and H4.

252

### 253 3.3.4. Core SU90-38

254 The ‘detrital factor’ is significantly lower between 130 and 70 ka than between 70 and  
255 10 ka. It remains stable in the upper part of the core even during Heinrich events. The  
256 ‘smectite factor’ records more variations than the ‘detrital factor’, but they are not correlated  
257 with Heinrich events: the factor decreases during H6, increases slightly during H5, H4, and  
258 H2, whereas it does not vary during H1 (Fig. 4).

259 In summary, the Heinrich events are not characterized by any significant variations of  
260 the ‘detrital factor’ and ‘smectite factor’ in core SU90-38, located in the northeastern Atlantic  
261 basin. By contrast, some of the Heinrich events — H5, H4, H2, and H1 — are characterized  
262 by the increase of the ‘detrital factor’ in cores SU90-08, SU90-11 and SU90-12, which were  
263 taken from the northwestern Atlantic basin. The variations of the ‘detrital factor’ associated  
264 with the Heinrich events are better developed in the southernmost cores SU90-08 (43°N) and  
265 SU90-11 (44°N), than in the northernmost core SU90-12 (51°N). The ‘smectite factor’ does  
266 not show a consistent pattern of variations. In core SU90-08, the ‘smectite factor’ decreases  
267 during the Heinrich events H5, H4, H2, and H1. In the other cores, the variations of the  
268 ‘smectite factor’ are not the same during all Heinrich events. Variations in the ‘mixed-layer  
269 factor’ characterize only the westernmost cores SU90-11 and SU90-12. Sharp increases to  
270 maximum value are followed by rapid drops below average values in the Heinrich events H5,

271 H4, H2, and H1. In core SU90-12, the decrease of the 'mixed-layer factor ' is more drastic for  
272 H5 and H4.

273

#### 274 **4. Discussion**

275

##### 276 *4.1. Clay mineral sources*

277 Under present climatic conditions, the typical terrigenous clay minerals, illite and  
278 chlorite, mainly results from physical weathering of continental substrates at high latitudes  
279 (Biscaye, 1965; Griffin et al., 1968; Rateev et al., 1969; Millot, 1970; Lisitzin, 1972;  
280 Chamley, 1975; Chamley, 1989). During glacial times or when climatic conditions were  
281 colder, physical weathering was intensified, leading to greater rock fragmentation and  
282 disintegration, and therefore increasing the terrigenous input to the ocean (Chamley, 1989). In  
283 the northeastern Atlantic basin, the main sources of chlorite and illite are the Scandinavian  
284 shields, Scotland, Ireland and Greenland (Moyes et al., 1964; Biscaye, 1965; Griffin et al.,  
285 1968). In the northwestern Atlantic basin, chlorite and illite derive from the Precambrian and  
286 Paleozoic igneous and sedimentary rocks of the North American continent, Baffin Island, and  
287 Greenland (Piper and Slatt, 1977; Petersen and Rasmussen, 1980; Thiébault et al., 1989).

288 Kaolinite, in the northernmost Atlantic basin, is essentially inherited from adjacent  
289 land masses where it formed during pre-glacial times and is derived from pre-existing  
290 paleosols, sediments or sedimentary rocks on the continents (Darby, 1975; Naidu et al., 1982;  
291 Sancetta et al., 1985; Chamley, 1989; Thiébault et al., 1989). In the northeastern Atlantic  
292 basin, the sources of kaolinite are the Mesozoic areas around the Barents Sea (Kuhlemann et  
293 al., 1993) and southeastern Svalbard (Elverhøi, 1979). In the northwestern Atlantic basin,  
294 kaolinite could derive from sedimentary formations of the North American continent (Boyd  
295 and Piper, 1976; Piper and Slatt, 1977) such as the black Cretaceous mudstones of Labrador  
296 (Jennings, 1993).

297 The IVMLs are not commonly observed in sediments, and constitute a good  
298 discriminant for particle sources. They mainly result from moderate pedogenic processes  
299 during interglacial Quaternary conditions at mid- to high latitudes. They seem to result  
300 especially from the weathering of mica in an alkaline environment (Millot, 1970) or from  
301 pedogenic transformation in soils under temperate climatic conditions (Berry and Johns,  
302 1966). IVML main sources are from Tertiary sediments in Virginia (McCartan, 1988), the  
303 Canadian Appalachians Mountains (Yang and Hesse, 1991) and in the Adirondack  
304 Mountains, NY State (April et al., 1986). IVMLs form from pedogenic processes in the

305 Canadian Appalachians Mountains and are transported by run-off to the Labrador shelf area.  
306 IVML has been also identified as reworked material in fluvial sediments on the western coast  
307 of Greenland (Petersen and Rasmussen, 1980). Recent work (Fagel et al., 1996) in the  
308 Labrador basin demonstrates that IVMLs are abundant at shallow depth in Labrador shelf  
309 sediments (<300 m water depth). But their abundance decreases to traces at greater water  
310 depth and they have not been found yet in the deepest parts of the Labrador basin. At 2698 m  
311 off New Jersey (ODP Site 905A) IVML constitute 5–25% of the clay mineral association of  
312 Pleistocene sediments (Deconinck and Vanderaverroet, 1996). IVMLs are assumed to be  
313 inherited from ancient soils developed on nearby mica-rich schists (Rich, 1956).

314 Smectite is common in North Atlantic sediments. It results from the chemical  
315 alteration of basalts, volcanic ashes and glasses, from pedogenic evolution of illite, or from  
316 erosion of old sediments formed during intervals when local climatic conditions (warm and  
317 hydrolyzing) allow pedogenic formation of smectite (Desprairies and Bonnot-Courtois, 1980;  
318 Chamley, 1989). Iceland, the Faeroe Islands (Parra et al., 1985), and the North European  
319 continental Tertiary formations, constitute the main sources of smectite in the northeastern  
320 Atlantic basin. Smectite is less abundant in the northwestern Atlantic basin, because of greater  
321 distance from the main continental sources (Berthois et al., 1973; Grousset, 1983; Grousset  
322 and Chesselet, 1986), or because climatic conditions in adjacent continental areas were too  
323 cold to allow pedogenic formation of smectite during the Quaternary. Nevertheless, smectite  
324 represents 5–50% of the clay mineral association in the Labrador Sea (Nielsen et al., 1989;  
325 Thiébault et al., 1989; Fagel et al., 1996). The main sources of smectite in this area are the  
326 northeastern Canadian Tertiary formations and smectite is also a main component in  
327 sediments off Cumberland Sound and Baffin Island (Jennings, 1993; Andrews et al., 1996;  
328 Jennings et al., 1996). Higher abundances of smectite at the rise/slope boundary on the path of  
329 the Western Boundary Under-Current could result from the mixture of particles transported  
330 from the Northern Labrador Sea and from the Iceland–Reykjanes ridge (Fagel et al., 1996).

331

#### 332 *4.2. Dynamics of the Heinrich events*

333 Clay minerals allow recognition of temporal variations in the characteristics of the  
334 Heinrich events in the following ways:

- 335 – In the northeastern Atlantic basin, Heinrich layers, which are otherwise characterized  
336 by an increased coarse fraction, are not characterized by any variation of the clay  
337 mineral association. By contrast, in the northwestern Atlantic basin, most of the

338 Heinrich layers are also characterized by important modifications in the clay mineral  
339 associations.

- 340 – The Heinrich layers of the North West Atlantic are enriched in ‘detrital’ clay minerals  
341 (i.e. illite C chlorite C kaolinite) especially in the southern cores SU90-08 (43°N) and  
342 SU90-11 (44°N). However, the more recent Heinrich layers (H1 and H2) of the  
343 northernmost core SU90-12 do not show any enrichment in detrital clay minerals.
- 344 – Increased supply of detrital clay minerals is especially obvious in H1 (14.5 ka), H2  
345 (22 ka), H4 (40 ka), and H5 (50 ka). Only slight increases are observed in H3 (27 ka)  
346 and H6 (60 ka) (the ‘detrital factor’ slightly increases).

347 Since illite, chlorite, and kaolinite all increase simultaneously during the Heinrich events,  
348 their input probably result from the same mechanism. This mechanism starts abruptly as  
349 shown by the rapid increase of the ‘detrital factor’ at the beginning of the Heinrich events.  
350 Chlorite, illite, and kaolinite, in the northwestern Atlantic basin, derive from the erosion of  
351 Precambrian/Paleozoic igneous rocks (Piper and Slatt, 1977; Thiébaud et al., 1989) and  
352 Paleozoic/Cretaceous sedimentary rocks of the north American continent, especially in the  
353 Labrador and Baffin Bay area (Boyd and Piper, 1976; Jennings, 1993). According to the main  
354 actual surface-water circulation pattern in the western basin (Fig. 1), an ice-rafting mechanism  
355 is then assumed to be responsible for the enhanced supply of detrital clay minerals as for  
356 detrital carbonates (Andrews and Tedesco, 1992; Bond et al., 1992; Grousset et al., 1993). A  
357 logical model is as follows: during the growth of the Laurentide ice-sheet, its base eroded the  
358 sedimentary formations and bedrock of the Canadian Shield, and consequently glacially  
359 reworked detrital carbonates (calcite and dolomite) and detrital clay minerals were transported  
360 into the ice to the shelf area. There, fragmentation of the ice-sheet released icebergs  
361 containing detrital clay minerals, which followed the main surface circulation pattern  
362 (Labrador Current) to the North Atlantic ocean (Fig. 1). During their southern transfer, the  
363 icebergs began to melt and progressively discharged their detrital load. The northernmost  
364 cores (SU90-11 and SU90-12) are located on seamounts, 1000 m above the sea floor, so  
365 bottom currents cannot be involved in particle transport to these sites. Close association of  
366 increased detrital clays with sand-sized ice-rafted particles at site SU90-11 suggest that  
367 sedimentation processes involved ice melting. Melting accelerated when icebergs reached  
368 warmer waters near the polar front, and changed direction to follow the North Atlantic Drift,  
369 increasing the incorporation of ice-rafted particles (including detrital clays) to the sediment.

370 The Heinrich events are also characterized by:

- 371 – An increased supply of IVML supply in (39°W), whereas IVMLs are absent from the  
372 eastern Atlantic basin and in the eastern part of the northwestern Atlantic basin (core  
373 SU90-08, 30°W). The comparison between the variations of both ‘detrital’ and  
374 ‘mixed-layer’ factors in cores SU90-11 and SU90-12 indicates that increased supply  
375 of mixed-layer supply precedes deposition of typically detrital clay minerals.  
376 Moreover, IVML supply stops before detrital clays began to decrease. It suggests (1)  
377 that two different mechanisms are involved, and (2) that the IVML supply results from  
378 a mechanism more rapid than those responsible for the supply of illite, chlorite, and  
379 kaolinite.
- 380 – Increased supply of IVML also occurs in the two more recent Heinrich events (H1 and  
381 H2) of core SU90-12 where there is no evidence of any increased detrital ice-rafted  
382 clays.

383 All this evidence indicates that IVMLs have not been transported by ice like detrital  
384 carbonates and detrital clay minerals. Moreover, the specific location of the cores SU90-11  
385 and SU90-12 (on seamounts, 1000 m above the sea floor) prevents particle transport to these  
386 sites by bottom currents. These minerals may be carried either by deep to intermediate water  
387 masses or by eolian circulation. Comparison of the distribution of the IVML in the  
388 northwestern Atlantic basin and of the main atmospheric circulation pattern is not consistent  
389 with an eolian supply (Bout-Roumazeilles, 1995). Therefore, intermediate to deep water-  
390 circulation may be responsible for the supply of the mixed-layer clays during the Heinrich  
391 events. This supply could be associated to the mechanism of the Labrador nepheloid layer  
392 (Eittrheim et al., 1969; Eittrheim and Ewing, 1974; Biscaye and Eittrheim, 1974, 1977) or to ice-  
393 shelf flow (Hulbe, 1997). Ice-flow during fragmentation of ice caps and release of icebergs  
394 eroded surface sediments of the continental shelves. In the Labrador Sea, these shallow  
395 sediments are enriched in IVML (Bout-Roumazeilles, 1995; Fagel et al., 1996), formed  
396 through pedogenic processes and transported to the shelf area by run-off during interglacials  
397 (Fig. 7). These particles contribute to the formation of a nepheloid layer which flows at  
398 intermediate depth because of relatively high density. Increased fragmentation of the  
399 Labrador ice sheet during some Heinrich events (H1, H2, H4 and H5) may have resulted in  
400 intensified erosion of IVML-rich surface sediments on the shelf. Increased IVML appears  
401 directly linked to ice-sheet dynamics. Increases of both ice-rafted detritus and IVML  
402 characterizes the Heinrich events but they are not closely dependent (Fig. 6). This suggests  
403 variations of ice-sheet dynamics in relation to climate, which need further investigations.

404

### 405 *4.3. Spatial distribution of the nepheloid layer*

406 Extension of the nepheloid layer can be estimated by comparison of mineralogical  
407 data from subsurface sediments at various depths, latitudes and longitudes of the northwestern  
408 Atlantic (Table 7). The database includes the Paleocinat I cruise mineralogical data (Bout-  
409 Roumazeilles, 1995), and mineralogical results (Fagel et al., 1996) from the Labrador Sea and  
410 the North Atlantic Ocean (cruises Hudson 90 and 91).

411 The IVMLs are abundant at shallow water depth (301 to 530 m) of the southern  
412 Labrador shelf (cores 1, 2, and 3, Table 7). They decrease at deeper water depth: 5% in core 4  
413 (1364 m), trace amounts in cores 5 (1984 m) and 6 (2648 m). These results indicate that the  
414 nepheloid layer formed in shallow areas, especially off southern Labrador. The presence of  
415 IVML in subsurface sediments from seamounts east of the shelf (cores 90-13 and SU90-12)  
416 provides evidence of the main southeastward direction of the nepheloid layer (Fig. 7).  
417 However, it is surprising not to find IVML in core 7 nor in cores 25, 27, and 28 (Fagel et al.,  
418 1996). This could result from the deep location of these cores (between 3378 and 3992 mbsf),  
419 but in this case it is difficult to explain the presence of IVML in core SU90-11 (3645 mbsf).  
420 Nevertheless the northern edge of the nepheloid layer is roughly situated near 57°N. This edge  
421 is related to the position of the intermediate- to deep-water current, which flows from the  
422 Irminger basin to the Labrador basin off southern Greenland. IVMLs have not been reported  
423 from the northeastern Atlantic basin. The analysis of the clay mineral fraction from cores  
424 9003, 9005, 9006, 9009, 9010, and SU90-08 does not reveal any traces of IVML in  
425 subsurface sediments. This indicates that the eastern edge of the nepheloid layer (Fig. 7) is  
426 situated somewhere between 39°W (core SU90-12) and 34°W (core 9010). Hence it appears  
427 that the mid-oceanic ridge acts as a barrier to prevent the extension of the nepheloid layer into  
428 the northeastern Atlantic basin. The nepheloid layer flows southward, following the pattern of  
429 deep circulation (Fig. 7) and carrying IVML to the latitude of New Jersey at least (Deconinck  
430 and Vanderaveret, 1996).

431

## 432 **5. Conclusions**

433 (1) Most Heinrich events of the northwest Atlantic Ocean are characterized by major  
434 modifications of the clay minerals association and incorporation of clay-size ice-rafted  
435 particles to the sediments:

436 (a) Heinrich events H1, H2, H4, and H5 are enriched in illite, chlorite, and kaolinite.  
437 Illite and chlorite are typically detrital clay minerals resulting from glacial erosion. In the

438 northwestern Atlantic basin, they mainly derive from the Precambrian and Paleozoic igneous  
439 and sedimentary rocks of the North American continent (Piper and Slatt, 1977; Thiébault et  
440 al., 1989). In the northwestern Atlantic basin, kaolinite is derived from adjacent landmasses  
441 where it formed during pre-glacial or interglacial periods, and from old sedimentary  
442 formations (such as the black Cretaceous mudstones of Labrador (Boyd and Piper, 1976;  
443 Jennings, 1993).

444 (b) The Heinrich layers are also enriched in IVML, which formed during interglacial  
445 periods through pedogenic processes (Berry and Johns, 1966). In the northwestern Atlantic  
446 basin, these minerals have been transported by run-off during interglacial periods from the  
447 Canadian Appalachian Mountains (Yang and Hesse, 1991) to the Labrador shelf (Fagel et al.,  
448 1996).

449 (2) Clay mineral studies show that the Heinrich layers do not only result from an ice-  
450 rafting mechanism, and the dynamic of their formation is complex and results from at least  
451 two important mechanisms:

452 (a) Detrital carbonates and typically detrital clay minerals (illite C chlorite C kaolinite)  
453 are carried and discharged by icebergs during disintegration of the Laurentide ice-sheet.

454 (b) The enhanced supply in IVML results from the erosion of the shelf during  
455 formation of a dense nepheloid layer flowing at an intermediate water depth, and following  
456 the general pattern of intermediate and deep-water circulation. Such a nepheloid layer is  
457 seasonally documented in the modern Labrador Sea (Eittrheim et al., 1969; Eittrheim and  
458 Ewing, 1974; Biscaye and Eittrheim, 1974, 1977). Andrews and Tedesco (1992) first proposed  
459 its contribution to the Heinrich deposits on the basis of high sedimentation rates. This  
460 mechanism is more rapid, and at least as important as ice-rafting discharges, because of the  
461 huge amounts of particles transported in a very short time. The extension of the nepheloid  
462 layer is determined by comparison of mineralogical analyses of subsurface sediments from  
463 different cores. The nepheloid layer forms in shallow areas and flows eastward along the  
464 slope and in the basin at intermediate water depth, to the mid-oceanic ridge which prevents  
465 penetration of the nepheloid layer into the northeastern Atlantic basin. The current flows  
466 principally southward, following the main pattern of deep-water circulation.

467 (3) Comparison between the variations of IVML and of illite C chlorite C kaolinite,  
468 indicates that increased mixed-layer supply by the nepheloid precedes the detrital clay supply  
469 by ice-rafting processes. The nepheloid layer formation and ice-rafting processes do not  
470 depend directly from each other. Nevertheless, ice-sheet dynamics are assumed to be  
471 responsible for both mechanisms. This implies that ice-sheet dynamics are more complex than

472 previously thought, and that they strongly control the transport of fine particles to the ocean.  
473 Therefore, clay minerals could be used as markers for further investigations of the dynamics  
474 of ice-sheets.

475

#### 476 **Acknowledgements**

477 We are grateful to Philippe Récourt for technical assistance. Review and constructive  
478 comments by C. Robert and K.T. Pickering are gratefully acknowledged. The coring cruise  
479 Paleocinat I of the French R/V *Le Suroît* was supported by Genavir and IFREMER. This  
480 work was financially supported by PNEDC from INSU, by the EEC program Environment  
481 and Climate (EV5V-CT92-0117) and by the URA 719 CNRS 'Sédimentologie et  
482 Géodynamique', Université de Lille 1.

483

#### 484 **References**

- 485 Albarède, F., 1995. Introduction to Geochemical Modeling. Cambridge Univ. Press, 543 pp.
- 486 Andrews, J.T., Tedesco, K., 1992. Detrital carbonate-rich sediments, northwestern Labrador  
487 Sea — implications for ice sheet dynamics and icebergs rafting (Heinrich) events in the north  
488 Atlantic. *Geology* 20, 1087–1090.
- 489 Andrews, J.T., Erlenkeuser, H., Tedesco, K., Aksu, A.E., Jull, A.J.T., 1994. Late Quaternary  
490 (stage 2 and 3) meltwater and Heinrich events, northwest Labrador Sea. *Quat. Res.* 41, 26–  
491 34.
- 492 Andrews, J.T., Osterman, L.E., Jennings, A.E., Syvitski, J.P.M., Miller, G.H., Weiner, N.,  
493 1996. Abrupt changes in marine conditions, Sunneshine fiord, eastern Baffin Island, NWT,  
494 during the last deglacial transition: Younger Dryas and H-0 events. In: Andrews, J.T., Austin,  
495 W.E.N., Bergsten, H., Jennings, A.E. (Eds.), Late Quaternary Palaeoceanography of the North  
496 Atlantic Margins. *Geol. Soc. Spec. Publ.* 111, 11–27.
- 497 April, R.H., Hluchy, M.M., Newton, R.M., 1986. The nature of vermiculite in Adirondack  
498 soils and till. *Clays Clay Miner.* 34 (5), 549–556.
- 499 Berry, R.W., Johns, W., 1966. Mineralogy of the clay-size fractions of some north-Atlantic  
500 Arctic Ocean bottom current. *Geol. Soc. Am. Bull.* 77, 183–196.
- 501 Berthois, L., Latouche, C., Parra, M., 1973. Etude minéralogiques et géochimiques de  
502 quelques sédiments de la zone comprise entre les archipels Faeroes, Shetland, Orcades et  
503 Hébrides. *Bull. Inst. Geol. Bassin Aquitaine* 14, 3–17.
- 504 Biscaye, P., 1965. Mineralogy and sedimentation of recent deep-sea clay in the Atlantic  
505 Ocean and adjacent seas and oceans. *Geol. Soc. Am. Bull.* 76, 803–832.

506 Biscaye, P., Eittreim, S.L., 1974. Variations in benthic boundary layer phenomenon:  
507 nepheloid layer in the North American basin. In: Gibbs, R.J. (Ed.), *Suspended Solids in*  
508 *Water*. Plenum Press, New York, NY, pp. 227–260.

509 Biscaye, P., Eittreim, S.L., 1977. Suspended particulate loads and transports in the nepheloid  
510 layer of the abyssal Atlantic Ocean. *Mar. Geol.* 23, 155–172.

511 Bond, G., Heinrich, H., Broecker, W., Labeyrie, L., McManus, J., Andrews, J., Huon, S.,  
512 Jantschick, R., Clasen, S., Simet, C., Tedesco, K., Klas, M., Bonami, G., Ivy, S., 1992.  
513 Evidence for massive discharges of icebergs into the North Atlantic Ocean during the last  
514 glacial period. *Nature* 360, 245–249.

515 Bout-Roumazeilles, V., 1995. Relations entre les variabilités minéralogiques et climatiques  
516 enregistrées dans les sédiments de l'Atlantique nord pendant les huit derniers stades  
517 glaciaires/interglaciaires. Thèse Univ. Lille I, 280 pp.

518 Boyd, R.W., Piper, D.J.W., 1976. Baffin Bay continental shelf clay mineralogy. *Marit.*  
519 *Sediment.* 12 (1), 17–18.

520 Broecker, W., Bond, G., Klas, M., Clark, E., McManus, J., 1992. Origin of the northern  
521 Atlantic's Heinrich events. *Clim. Dyn.* 6, 265–279.

522 Chamley, H., 1975. Remarque sur la sédimentation argileuse quaternaire en Mer de Norvege.  
523 *Union Océanogr. Fr.* 7, 15– 20.

524 Chamley, H., 1989. *Clay Sedimentology*. Springer, Berlin, 623 pp.

525 Cortijo, E., Reynaud, J.Y., Labeyrie, L., Paillard, D., Lehman, B., Cremer, M., Grousset, F.,  
526 1995. Etude de la variabilité climatique à haute résolution dans des sédiments de l'Atlantique  
527 Nord. *C. R. Acad. Sci. Ser. II* 321, 231–238.

528 Darby, S.A., 1975. Kaolinite and other clay minerals in Arctic Ocean sediments. *J. Sediment.*  
529 *Petrol.* 45, 272–279.

530 Deconinck, J.F., Vanderaveroet, P., 1996. Eocene to Pleistocene clay mineral sedimentation  
531 off New-Jersey, western north Atlantic (ODP Leg 150, sites 903 and 905). *Proc. ODP Sci.*  
532 *Results* 150, 147–170.

533 Desprairies, A., Bonnot-Courtois, C., 1980. Relation entre la composition des smectites  
534 d'alteration sous-marine et leur cortège de terres rares. *Earth Planet. Sci. Lett.* 48, 124–130.

535 Dickson, R.R., Brown, J., 1994. The production of North Atlantic Deep Water: sources, rates  
536 and pathways. *J. Geophys. Res.* 99, 12319–12341.

537 Eittreim, S.L., Ewing, M., 1974. Turbidity distribution in the deep waters of the western  
538 Atlantic trough. In: Gibbs, R.J. (Ed.), *Suspended Solids in Water*. Plenum Press, New York,  
539 NY, pp. 213–225.

540 Eittrheim, S., Ewing, H., Thorndike, E.M., 1969. Suspended matter along the continental  
541 margin of the North American basin. *Deep-Sea Res.* 16, 613–624.

542 Elverhøi, A., 1979. Sedimentological and mineralogical investigations of quaternary bottom  
543 currents off the Norwegian West Coast. *Nor. Geol. Tidsskr.* 59, 273–284.

544 Fagel, N., Robert, C., Hillaire-Marcel, C., 1996. Clay mineral signature of the NW Atlantic  
545 Boundary Undercurrent. *Mar. Geol.* 130, 19–28.

546 Griffin, J.J., Windom, H., Goldberg, E.D., 1968. The distribution of clay minerals in the  
547 world ocean. *Deep-Sea Res.* 15, 433–459.

548 Grousset, F., 1983. *Sédimentogénèse d'un environnement de dorsale: la ride Açores-Islande*  
549 *au cours du dernier cycle climatique. Origines, vecteurs, flux des particules sédimentaires.*  
550 *Thèse Univ. Bordeaux*, 232 pp.

551 Grousset, F., Chesselet, R., 1986. The Holocene sedimentary regime in the northern mid-  
552 Atlantic ridge region. *Earth Planet. Sci. Lett.* 78, 271–287.

553 Grousset, F.E., Labeyrie, L., Sinko, J.A., Cremer, M., Bond, G., Duprat, J., Cortijo, E., Huon,  
554 S., 1993. Patterns of ice-rafted detritus in the glacial north Atlantic (40°-55°N).  
555 *Palaeoceanography* 8 (2), 175–192.

556 Heinrich, H., 1988. Origin and consequences of cyclic ice-rafting in the northeast Atlantic  
557 Ocean during the past 130,000 years. *Quat. Res.* 29, 142–152.

558 Holtzapffel, T., 1985. *Les minéraux argileux. Préparation. Analyse diffractométrique et*  
559 *détermination. Mem. Soc. Geol. Nord, Lille* 12, 136 pp.

560 Hulbe, C.L., 1997. An ice shelf mechanism for Heinrich layer production. *Palaeoceanography*  
561 12 (5), 711–717.

562 Huon, S., Ruch, P., 1992. Mineralogical, K-Ar, and <sup>86</sup>Sr/<sup>87</sup>Sr isotopes study of Holocene and  
563 late glacial sediment in a deep-sea core from northeast Atlantic Ocean. *Mar. Geol.* 107 (4),  
564 275–282.

565 Jennings, A.E., 1993. The Quaternary history of Cumberland Sound, southeastern Baffin  
566 Island: the marine evidence. *Géogr. Phys. Quat.* 47, 21–42.

567 Jennings, A.E., Tedesco, K.A., Andrews, J.T., Kirby, M.E., 1996. Shelf erosion and glacial  
568 ice proximity in the Labrador Sea during and after Heinrich events (H-3 or 4 to H-0) as shown  
569 by foraminifera. In: Andrews, J.T., Austin, W.E.N., Bergsten, H., Jennings, A.E. (Eds.), *Late*  
570 *Quaternary Palaeoceanography of the North Atlantic Margins. Geol. Soc. Spec. Publ.* 111,  
571 29–49.

572 Johnson, R.A., Wichern, D.W., 1982. *Applied Multivariate Statistical Analysis.* Prentice-Hall,  
573 Englewood Cliff, NY, 285 pp.

574 Kuhlemann, J., Lange, H., Paetsch, H., 1993. Implications of a connection between clay  
575 mineral variations and coarse-grained debris and lithology in the central Norwegian-  
576 Greenland Sea. *Mar. Geol.* 114, 1–11.

577 Lisitzin, A.P., 1972. Sedimentation in the world ocean. *Soc. Econ. Paleontol. Mineral. Spec.*  
578 *Publ. Tulsa*, 218 pp.

579 Lucotte, M., Hillaire-Marcel, C., 1994. Identification des grandes masses d'eau dans les mers  
580 du Labrador et d'Irminger. *Can. J. Earth Sci.* 31, 5–13.

581 MacAyeal, D.R., 1993. Binge/purge oscillations of the Laurentide ice sheet as a cause of the  
582 North Atlantic's Heinrich events. *Palaeoceanography* 8 (6), 775–784.

583 Martinson, D.G., Pisias, N.G., Hays, J.D., Imbrie, J., Moore, T.C., Shackleton, N.J., 1987.  
584 Age dating and the orbital theory of ice-ages: Development of high resolution 0 to 300 000-  
585 year chronostratigraphy. *Quat. Res.* 27, 1–29.

586 McCartan, L., 1988. Mineralogy of the Haynesville, Virginia, cores. *U.S. Geol. Surv. Prof.*  
587 *Pap.* 1489, B1–B9.

588 McCave, I.N., Tucholke, B.E., 1986. Deep current-controlled sedimentation in the western  
589 North Atlantic. In: Vogt, P.R., Tucholke, B.E. (Eds.), *The Geology of North America, Vol.*  
590 *M, The Western North Atlantic Region.* Geological Society of America, Boulder, CO, pp.  
591 451–468.

592 Millot, G., 1970. *Geology of Clays.* Springer, Berlin, 425 pp.

593 Moyes, J., Duplessy, J.C., Gonthier, E., Latouche, C., Maillet, N., Parra, M., Pujol, C., 1964.  
594 Les sédiments profonds actuels et pléistocène récent de l'Atlantique nord-oriental et du sud de  
595 la Mer de Norvège. *IIeme Colloque international sur l'exploitation des océans, Bordeaux, 4,*  
596 *p.* 201.

597 Naidu, A.S., Creager, J.S., Mowatt, T.C., 1982. Clay mineral dispersal patterns in the north  
598 Bering and Chukchi Seas. *Mar. Geol.* 47, 1–5.

599 Nielsen, O.B., Cremer, M., Stein, R., Thiebault, F., Zimmerman, H., 1989. Analysis of  
600 sedimentary facies, clay mineralogy, and geochemistry of the paleogene sediments of site  
601 647, Labrador Sea. *Proc. ODP Sci. Results* 105, 101–110.

602 Paillard, D., Labeyrie, L., Yiou, P., 1996. Analyseries 1.0: a Macintosh software for the  
603 analysis of geographical time-series. *EOS* 77, 379.

604 Parra, M., Delmont, P., Ferragne, A., Latouche, C., Puechmaille, C., 1985. Origin and  
605 evolution of smectites in recent marine sediments of the NE Atlantic. *Clay Miner.* 20, 335–  
606 345.

607 Petersen, L., Rasmussen, K., 1980. Mineralogical composition of the clay-size fraction of two  
608 fluvio-glacial sediments from east Greenland. *Clay Miner.* 15, 135–145.

609 Piper, D.J.W., Slatt, R.M., 1977. Late Quaternary clay mineral distribution along the eastern  
610 margin of Canada. *Geol. Soc. Am. Bull.* 86, 267–272.

611 Rateev, M.A., Gorbunova, Z.N., Lisitzin, A.P., Nasov, G.L., 1969. The distribution of the  
612 clay minerals in the oceans. *Sedimentology* 13, 21–43.

613 Rich, C.I., 1956. Muscovite weathering in a soil developed in the Virginia Piedmont. *Clays*  
614 *Clay Miner.* 16, 15–36.

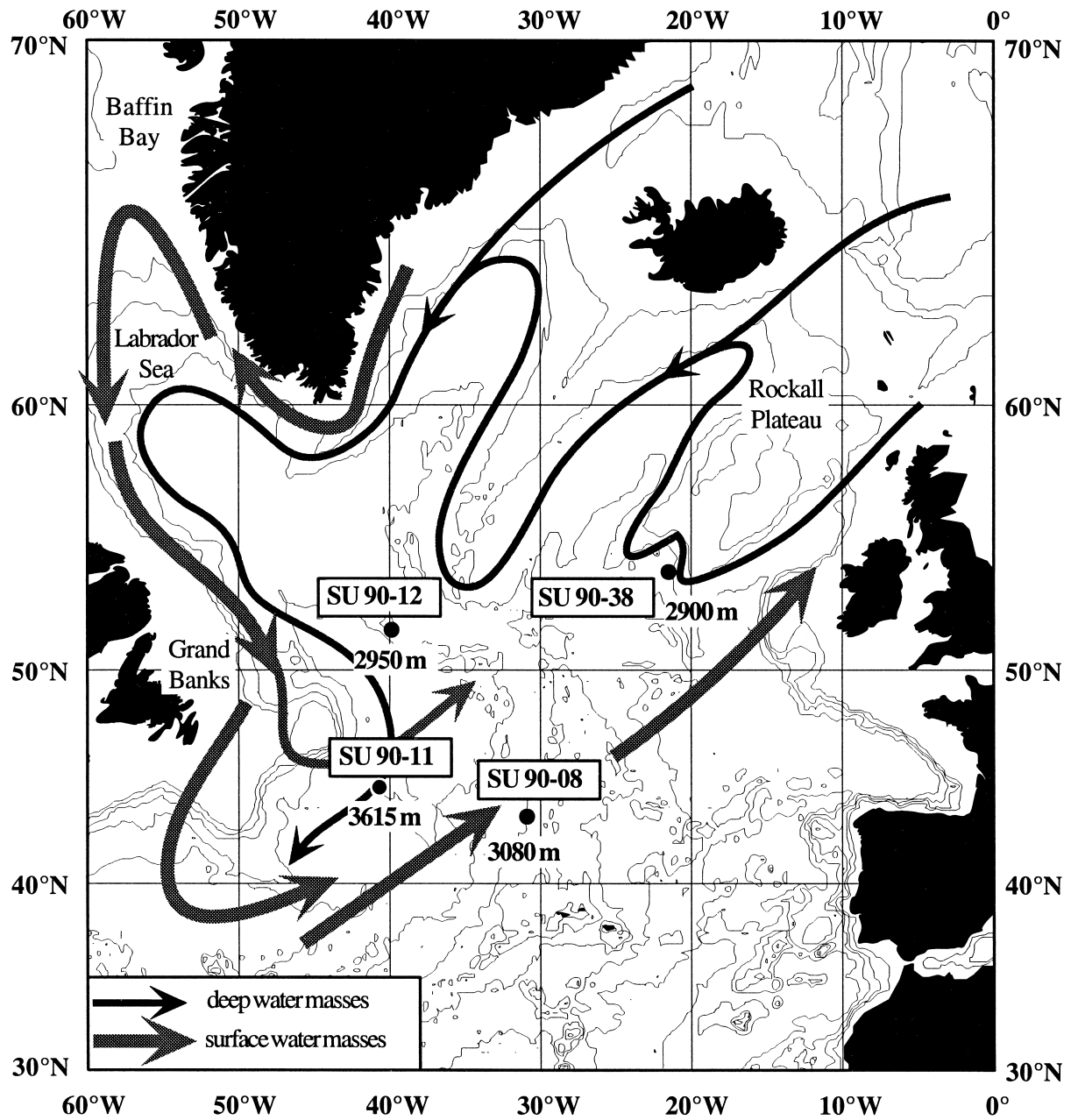
615 Ruddiman, W.F., 1977. Late Quaternary deposition of ice-rafted sand in the sub-polar north  
616 Atlantic (lat. 40° to 65°N). *Geol. Soc. Am. Bull.* 88, 1813–1827.

617 Sancetta, C., Heusser, L., Labeyrie, L., Naidu, A.S., Robinson, S.W., 1985. Wisconsin-  
618 Holocene paleoenvironment of the Bering Sea: evidence from diatoms, pollen, oxygen  
619 isotopes and clay minerals. *Mar. Geol.* 62, 55–68.

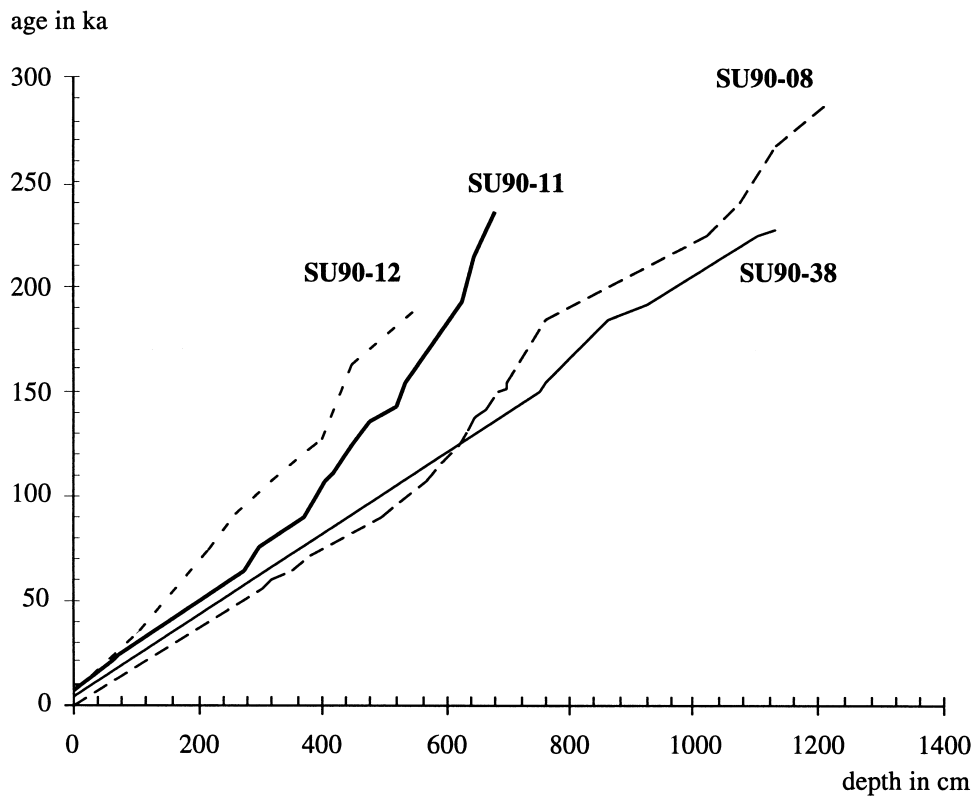
620 Thiébault, F., Cremer, M., Debrabant, P., Foulon, J., Nielsen, O.B., Zimmerman, H., 1989.  
621 Analysis of sedimentary facies, clay mineralogy, and geochemistry of the Neogene-  
622 Quaternary sediments in site 645, Baffin Bay. *Proc. ODP Sci. Results* 105, 83–100.

623 Yang, C., Hesse, R., 1991. Clay minerals as indicators of diagenetic and anchimetamorphic  
624 grade in an overthrust belt, external domain of southern Canadian Appalachians. *Clay Miner.*  
625 26, 211–231.

626



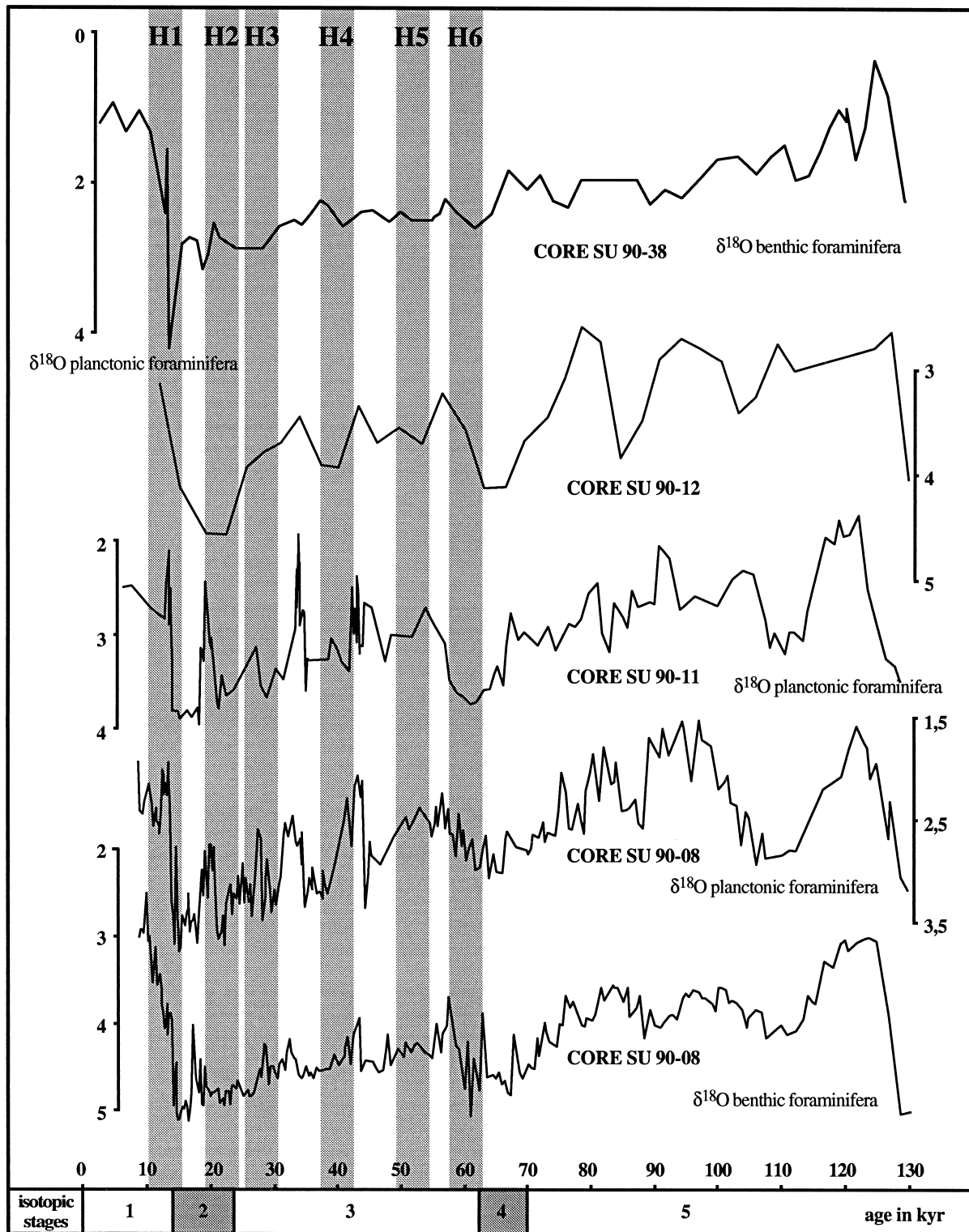
628  
629 Fig. 1. Study area, cores location and main deep and surface circulation patterns modified  
630 from McCave and Tucholke (1986), Dickson and Brown (1994) and Lucotte and Hillaire-  
631 Marcel (1994).  
632



633

634 Fig. 2. Age–depth relation for the studied cores.

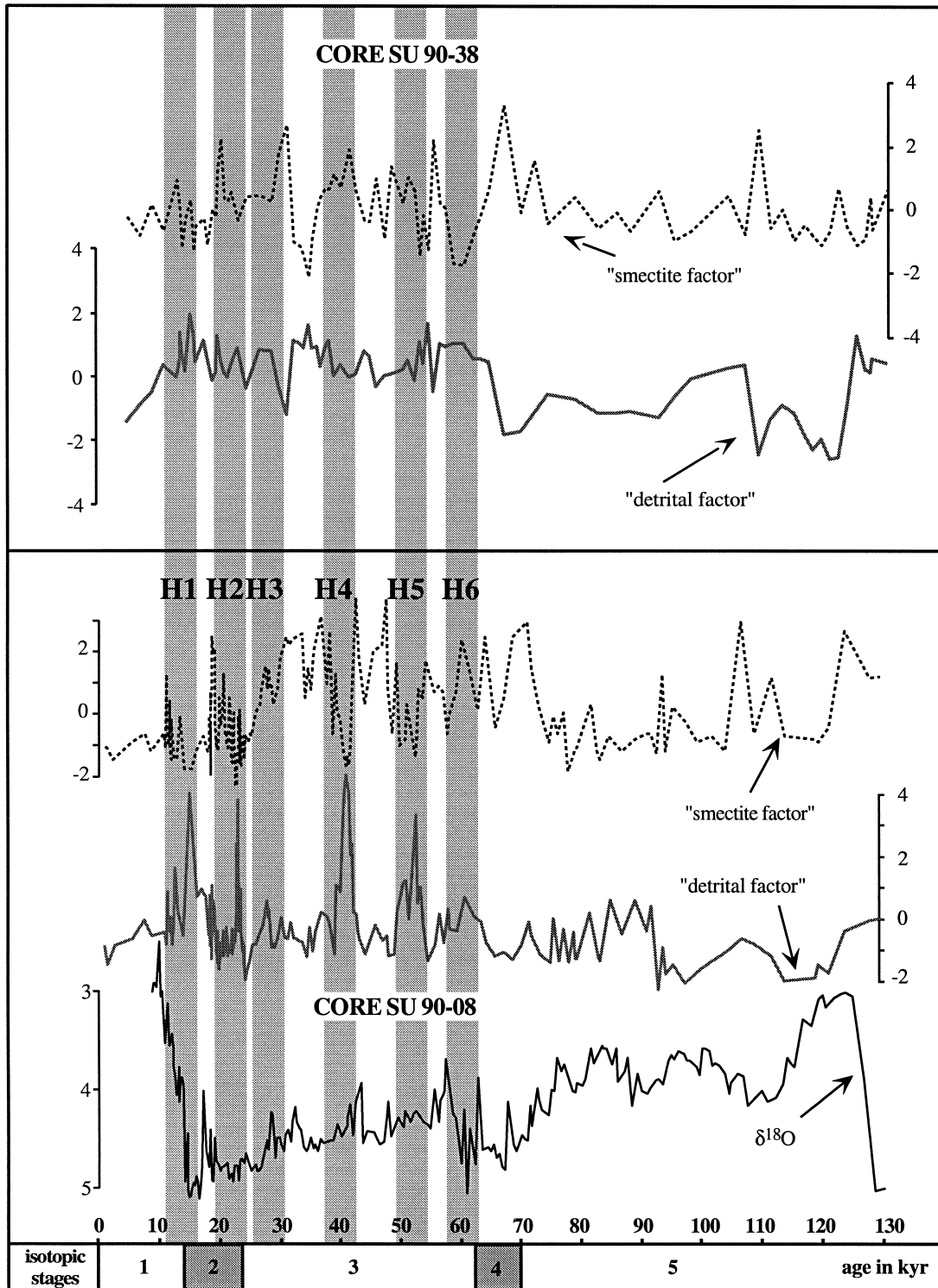
635



636

637 Fig. 3.  $\delta^{18}\text{O}$  on benthic and planktonic foraminifera of cores SU90-08, SU90-11, SU90-12  
 638 and SU90-38. The Heinrich layers are indicated by gray rectangles.

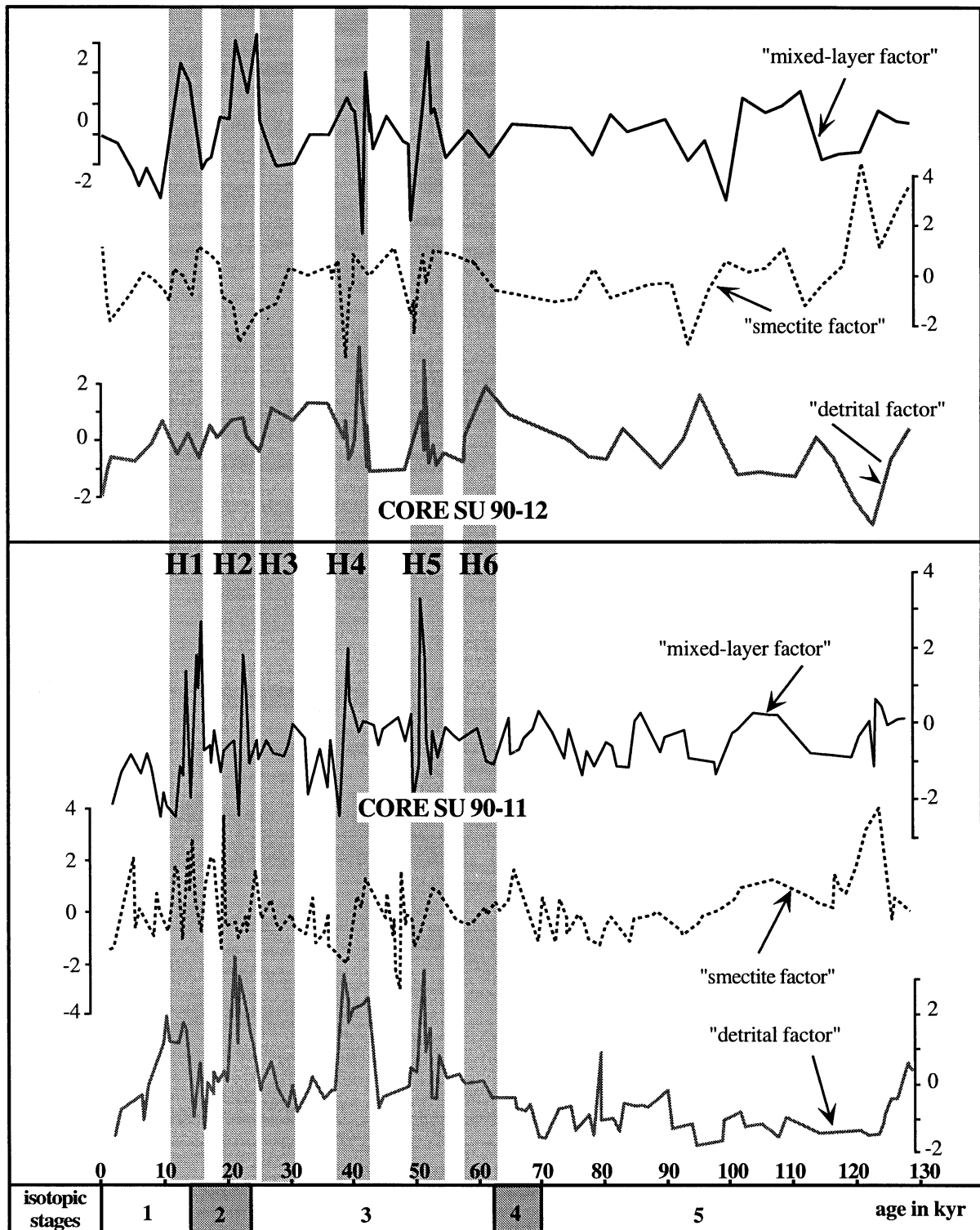
639



640

641 Fig. 4. Variations of the detrital (gray line) and smectite factors (dashed line), and  $\delta^{18}\text{O}$  on  
 642 benthic foraminifera over the last 130 kyr for cores SU90-08 (lower). Variations of the  
 643 detrital and smectite factors over the last 130 kyr for core SU90-38 (upper). Heinrich Events  
 644 *H1* to *H6* are indicated by gray rectangles.

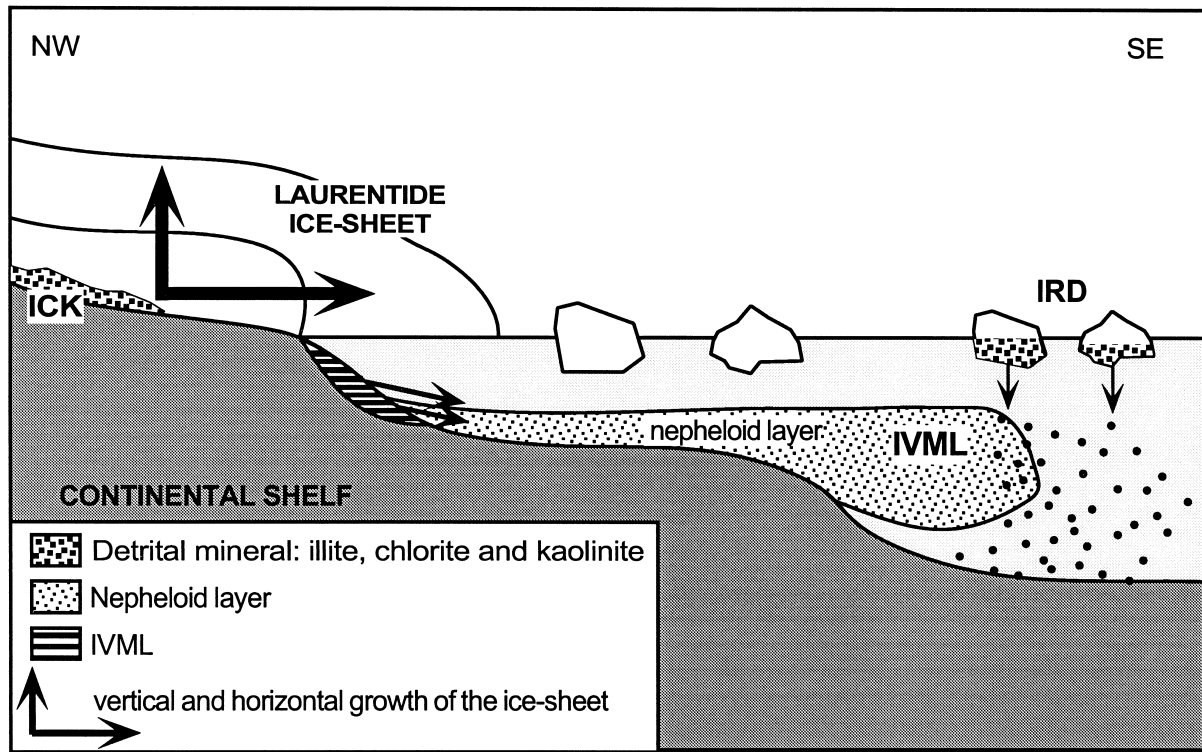
645



646

647 Fig. 5. Variations of the detrital (gray line), smectite (dashed line), and mixed-layer (solid  
 648 line) over the last 130 kyr for cores SU90-11 (lower) and SU90-12 (upper). Heinrich Events  
 649 *H1* to *H6* are indicated by gray rectangles.

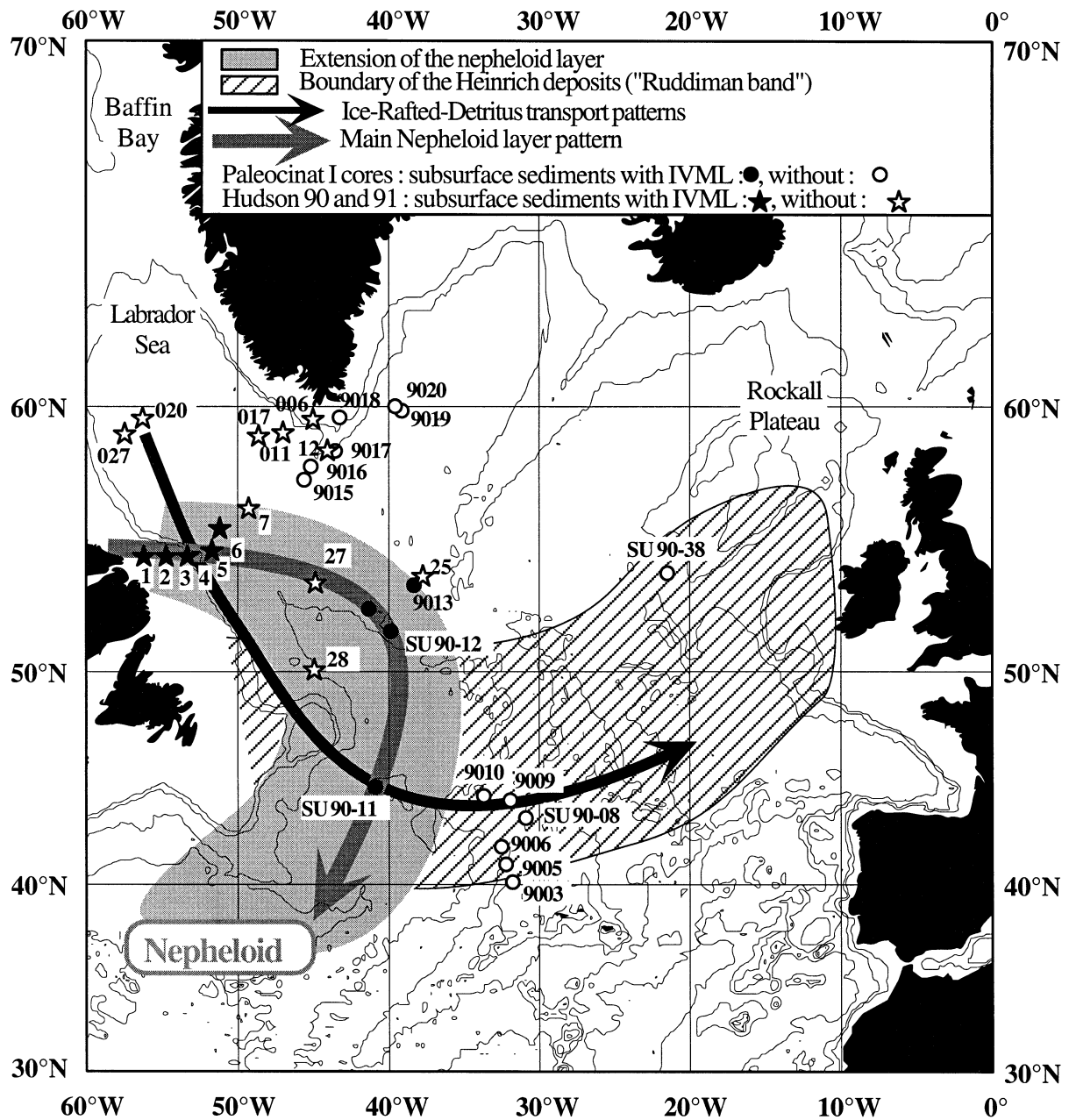
650



651

652 Fig. 6. Nepheloid layer and Ice-Rafted-Detritus transportation mechanisms since the Labrador  
 653 continental shelf area toward the open ocean during the Heinrich events, in relation with the  
 654 vertical and horizontal growth of the Laurentide ice-sheet. *ICK* = detrital minerals: illite,  
 655 chlorite, and kaolinite. *IVML* = illite-vermiculite mixed-layer red clay.

656



657

658 Fig. 7. Main sub-actual extension of the nepheloid layer main surface and IRD transportation  
 659 patterns according to clay mineral analyses from Paleocinat I cores 9003 to 9020 (Bout-  
 660 Roumazeilles, 1995) and from Hudson 90–91 cores (Fagel et al., 1996).

661

662 Table 1

663 Core characteristics

Cores	Latitude (N)	Longitude (W)	Depth (mbsf)	Length (m)
SU90-08	43°41'2	30°24'5	3080	12.27
SU90-11	44°43'6	40°15'8	3645	6.97
SU90-12	51°52'6	39°04'9	2950	15.5
SU90-38	54°05'4	21°04'9	2900	11.42

664

665

666 Table 2

667 Age–depth relation for the studied cores

SU90-08		SU90-11		SU90-12		SU90-38	
depth (cm)	age (ka)	depth (cm)	age (ka)	depth (cm)	age (ka)	depth (cm)	age (ka)
0	0	2.5	6	29.5	11.4	0	4.1
302	54.8	63	22	104	33.2	750	150.4
320	57.6	75	24	109	35.6	760	152.3
352	64.1	273	65	220.5	73.2	860	183.4
383	71.1	300	75	258.5	90.9	920	191.4
497	90.1	370	90	319.5	107.5	1100	225.2
526	96.4	404	107	380	122.2	1130	228.3
569.5	107.6	417.5	112	398.5	126.6		
589.5	115.9	445	125	448	162.8		
620	125	480	135	547.5	188.3		
633.5	131.1	520	143				
644.5	136.6	534	155				
653	139	624.5	193				
667	141.3	642.5	215				
685	149.3	677	237				
698.5	152.1						
699	152.6						
759	183.4						
1019	225.2						
1071	240.2						
1130	267.5						
1210	288.5						

668

669 Table 3

670 Mean clay mineral composition (%) and standard deviation (Sd) of sediments from the  
 671 studied cores without Heinrich layers data

Clay minerals	SU90-08		SU90-11		SU90-12		SU90-38	
	average	Sd	average	Sd	average	Sd	average	Sd
Chlorite	14	±3	20	±4	21	±4	14	±3
Illite	37	±7	34	±4	34	±5	39	±7
10-14s	6	±2	Tr.	-	-	-	-	-
10-14v	-	-	17	±7	18	±8	-	-
Smectite	33	±11	16	±7	15	±8	35	±11
Kaolinite	11	±3	12	±2	12	±2	11	±2
$\Sigma(I + C + K)$	62		66		67		64	

10-14s = illite-smectite mixed-layer minerals; 10-14v = illite-vermiculite mixed-layer minerals.

672

673

674 Table 4

675 Mean clay mineral composition (%) and standard deviation (Sd) of Heinrich layers sediments  
 676 from the studied cores

Clay minerals	SU90-08		SU90-11		SU90-12		SU90-38	
	average	Sd	average	Sd	average	Sd	average	Sd
Chlorite	20	±2	20	±2	19	±2	14	±2
Illite	55	±6	40	±4	42	±5	42	±5
10-14s	-	-	-	-	-	-	-	-
10-14v	-	-	28	±8	32	±11	-	-
Smectite	10	±2	-	-	8	±2	32	±4
Kaolinite	15	±2	12	±4	11	±3	12	±3
$\Sigma(I + C + K)$	90		72		60		68	

10-14s = illite-smectite mixed-layer minerals; 10-14v = illite-vermiculite mixed-layer minerals.

677

678

679 Table 5  
 680 Correlation matrix between clay minerals species for the studied cores

Cores	Clay minerals	Chlorite	Illite	10-14v	Smectite	Kaolinite
SU90-08	chlorite	1				
	illite	0.8	1			
	smectite	0.0	-0.0		1	
	kaolinite	0.8	0.7		0.0	1
SU90-11	chlorite	1				
	illite	0.8	1			
	10-14v	-0.0	-0.0	1		
	smectite	0.1	0.3	-0.6	1	
SU90-12	kaolinite	0.8	0.8	-0.2	0.4	1
	chlorite	1				
	illite	0.8	1			
	10-14v	-0.0	-0.1	1		
SU90-38	smectite	0.5	0.5	-0.5	1	
	kaolinite	0.7	0.8	-0.0	0.5	1
	chlorite	1				
	illite	0.9	1			
SU90-38	smectite	0.3	0.4		1	
	kaolinite	0.8	0.8		0.2	1

681 10-14v = illite-vermiculite mixed-layer minerals.

682

683 Table 6

684 Scores of the orthogonal transformation varimax solution (factor analysis) for the detrital,  
 685 smectite, and mixed-layer factors for the studied cores

Cores	Clay minerals	Detrital factor	Smectite factor	Mixed-layer factor
SU90-08	chlorite	0.9	0.0	
	illite	0.9	-0.0	
	smectite	0.0	1	
	kaolinite	0.9	0.0	
SU90-11	chlorite	0.9	-0.1	-0.0
	illite	0.9	0.1	0.0
	10-14v	-0.0	-0.3	0.9
	smectite	0.1	0.9	-0.3
SU90-12	kaolinite	0.9	0.3	-0.0
	chlorite	0.9	0.0	0.0
	illite	0.9	0.1	-0.0
	10-14v	-0.0	-0.1	1
SU90-38	smectite	0.4	0.8	-0.3
	kaolinite	0.8	0.3	0.0
	chlorite	0.9	0.1	
	illite	0.9	0.2	
SU90-38	smectite	0.1	1	
	kaolinite	0.9	0.0	

686 10-14v = illite-vermiculite mixed-layer minerals.

687

688 Table 7

689 Core characteristics, and 10-14v percentages in subsurface sediments

Cores	Lat. (N)	Long (W)	Depth (mbsf)	% 10-14v
9009	31°44'9	31°44'9	3370	–
9003	40°30'3	32°03'2	2475	–
9005	41°38'4	32°15'4	3285	–
9006	42°01'8	32°42'7	3510	–
SU90-08	43°31'2	30°24'5	3080	–
9010	44°42'1	34°42'3	3965	–
SU90-11	44°43'6	40°15'8	3645	26
28 <sup>a</sup>	50°12'2	45°41'1	3448	–
SU90-12	51°52'6	39°47'4	2950	20
9013	52°52'4	41°15'7	3660	5
27 <sup>a</sup>	53°19'7	45°15'6	3378	–
25 <sup>a</sup>	53°58'5	38°38'2	3603	–
2 <sup>a</sup>	54°44'5	55°35'0	301	35
3 <sup>a</sup>	54°49'2	53°43'9	340	27/tr
1 <sup>a</sup>	54°52'9	56°26'9	530	12
4 <sup>a</sup>	54°54'0	52°52'0	1364	5
5 <sup>a</sup>	55°02'0	52°44'7	1984	tr.
6 <sup>a</sup>	52°07'7	52°07'7	2648	tr.
7 <sup>a</sup>	56°36'9	49°45'0	3992	–
9014	57°39'2	46°51'2	2924	5
9015	57°58'5	45°54'8	2420	–
017 <sup>a</sup>	58°12'5	48°21'6	3379	–
9016	58°13'2	45°10'5	2100	–
020 <sup>a</sup>	58°21'5	57°27'3	2865	–
12 <sup>a</sup>	58°42'8	53°57'0	1559	–
027 <sup>a</sup>	58°45'7	57°05'1	3032	–
9017	58°47'8	43°57'0	1605	–
011 <sup>a</sup>	58°54'8	47°05'1	2805	–
9018	59°22'1	43°27'0	1015	–
006 <sup>a</sup>	59°29'4	45°52'2	1105	–
9019	59°32'2	39°27'8	2925	–
9020	59°51'7	39°39'8	2700	–

Cores 9003 to 9020 from Paleocinat I cruise (Bout-Roumzeilles, 1995).

<sup>a</sup> Cores from Hudson 90–91 cruises (Fagel et al., 1996).

690